Journal of Materials Chemistry B

Accepted Manuscript

ROYAL SOCIETY OF CHEMISTRY

www.rsc.org/materialsB

Journal Name

ARTICLE

A novel and facile approach to fabricate a conductive and biomimetic fibrous platform with sub-micron and micron features

Received 00th January 20xx,
Accepted 00th January 20xx

DOI: 10.1039/x0xx00000x

www.rsc.org/

Dorna Esrafilzadeh [ab], Rohoullah Jalili [a], Xiao Liu [a], Kerry J. Gilmore [a], Joselito M. Razal [ac], Simon E. Moulton [ad]*, Gordon G. Wallace [a]*

Demands of multifunctional scaffolds have exceeded the passive biocompatible properties previously considered suficient for tissue engineering. Herein, a novel and facile method used to fabricate a core-shell structure consisting of a conducting fiber core and an electrospun fiber shell is presented. This multifunctional structure simultaneously provides the high conductivity of conducting polymers as well as the enhanced interactions between cells and the sub-micron topographical environments provided by highly aligned cytocompatible electrospun fibers. Unlimited lengths of PEDOT:PSS-Chitosan-PLGA fibers loaded with an antibiotic drug, Ciprofloxacin hydrochloride, were produced using this method. The fibers provide modulated drug release with excellent mechanical properties, electrochemical performance and cytocompatibility, which hold great promise for the application of conductive electrospun scaffolds in regenerative medicine.

Introduction

One of the main challenges in tissue engineering is to design and fabricate an appropriate artificial 3D extracellular matrix (AECM) that is compatible with the physiologically relevant environment, so as to provide additional control over cell behavior.[1-4] In light of this need, many fabrication techniques have been developed to mimic the complex heterogeneous nature of natural tissues and organs for tissue engineering and regenerative medicine applications.[1] Fabrication strategies such as wet-spinning and electrospinning have been used to develop fibrous scaffolds with well-defined 3D topographies and geometries, from a range of biopolymers and biomolecules.[5-9]

Biocompatible fibers can be used to build biomimetic 3D scaffolds with tunable pore sizes, specific orientation and suitable mechanical strength.[10-12] Appropriate pore size can facilitate effective diffusion of nutrition, waste products, and gases within a 3D scaffold as well as allowing cell migration, spreading, and proliferation.[7, 11] It has been demonstrated that using AECM fabricated from sub-micron electrospun fibers enhances cell-materials interactions when compared to micron dimensional structures.[14] To this end, significant control over cell behavior including adhesion, proliferation, migration, and differentiation has been achieved using electrospun fibers.[13, 15, 16] Electrospinning of sub-micron fibers is a well-established and versatile technique used to produce fibers from a vast range of materials including conducting and non-conducting polymers.[13, 17-22] The diameter of electrospun fibers is typically in the sub-micron and nanometer size range and this can facilitate cellular interactions.[2, 3]

Additionally, scaffolds made from aligned electrospun fibers, as opposed to non-aligned electrospun fibers, provide more attractive substrates since cell alignment can be improved by the control over the separation, geometry and arrangement of the fibers.[6, 10, 23, 24] This positive effect is more pronounced when the AECM is designed to aid in regeneration of specific tissue types such as nerve, tendon or muscle, where the cells must be aligned in parallel to form the final tissue.[13, 23-25] In addition to mimicking the ECM, the migration and extension of cells can be driven by the orientation of electrospun fibers in a 3D scaffold. For example Schwann cell guidance using nano/microgrooved substrates has been reported by Tonazzini *et al.* for nerve repair applications.[26] Li *et al.* reported successful fabrication of gradients of stromal cell-derived factor-1α (SDF1α) on electrospun collagen mats using inkjet printing that led to neural progenitor stem cell migration toward the region with higher SDF1α content.[27]

Different techniques have been employed to control the alignment of electrospun fibers. These methods can be classified into three groups namely: mechanical, electrostatic, and magnetic, based on the nature of the forces utilized to control the collection of the electrospun fibers.[19-21, 28] In the case of mechanical force, a high speed-rotating take-up spool is commonly used to collect aligned electrospun fibers. The rotation speed of the take-up spool controls the degree of

[a] ARC Centre of Excellence for Electromaterials Science, Intelligent Polymer Research Institute, University of Wollongong, Wollongong, NSW 2522, Australia.
[b] Illawarra Health and Medical Research Institute, University of Wollongong, NSW, 2522, Australia.
[c] Current address: Deakin University, Geelong, Institute for Frontier Materials, VIC, 3220, Australia.
[d] Current address: Faculty of Science, Engineering and Technology, Swinburne University of Technology, Hawthorn, VIC, 3122, Australia.

alignment of the unidirectional non-woven material. Since electrostatic charges are carried by the electrospinning jet, manipulation of the electric/magnetic field can also be used to modify effective forces to the electrospun fibers just before their collection to control the alignment. The main limitation of these methods is that it is not possible to form continuous lengths of aligned/unidirectional electrospun fibers. Another challenge associated with aligned electrospun fibers is the ability to preserve the porosity of the final structure as the fibers are usually densely packed on the collecting spool. Aligned poly(l-lactic acid) (PLA) nanofibers have been used to successfully direct neurites sprouting from neonatal mouse cerebellum (C17.2 NSCs)[22] and aligned electrospun fibers have also been used to facilitate the healing process of scars by directing the migratory routes of cells in specific directions.[29] Tissue-like structures that have been developed using electrospun layers of poly-caprolactone (PCL) and collagen fibers, were fabricated with normal human dermal fibroblast (NHDF) cells injected between the layers to generate a layer-by-layer cell assembly. The cells remained within the different layers and were shown to form dermal-like tissues after one week of culture.[30]

Fabrication of AECM from conducting polymers can also offer intriguing platforms for tissue regeneration due to the ability to enhance cell growth via electrical stimulation, as well as to control the release of incorporated biological molecules.[5, 31-33] The release of pharmaceutical components or bioactive molecules can prevent acute or chronic responses after implantation and enhance cellular functions.[5, 34] Topographical design and cytocompatibility of the conducting AECM are critical factors that determine the degree of cell attachment and therefore, the capability to transfer electrical signals directly to the cells.[5, 31]

In the case of conducting polymers, wet-spinning has been used to produce macron-size fibers.[5, 35-37] The practical integration of electrically conductive wet-spun fibers with biomimetic electrospun fibers could enhance the development of conducting 3D scaffolds and facilitate their application in regenerative medicine. In this paper, we introduce a novel and facile method that enables unidirectional electrospun poly lactic-co-glycolic acid (PLGA) fibers to be coated onto micron dimensional conducting poly(3,4-ethylenedioxythiophene) poly(styrene sulfonate) (PEDOT:PSS) and Chitosan (CHI) (PEDOT:PSS-CHI) wet-spun fibers. The method outlined here can be used to spin unlimited lengths of aligned self-supported and oriented electrospun fibers. Cytocompatibility and cell interaction with the hybrid fibers have been assessed using the MTS cell viability assay, immunofluorescence staining of B35 neuroblastoma cells under proliferation and differentiation conditions as well as imaging of cells using a cryo-SEM technique. An antibiotic drug, Ciprofloxacin hydrochloride (Cipro), was incorporated into the hybrid fibers to provide localized antibiotic properties. The release of Cipro from these fibrous structures was also investigated.

Experimental

Materials

PEDOT:PSS pellets were obtained from Agfa (Orgacon dry, Lot A6 0000 AC). Ethanol (75%), dimethyl sulfoxide (DMSO) and paraformaldehyde (PFA), high molecular weight Chitosan (CHI) (M_w: 60,000-120,000), cyclic AMP (cAMP) and horse serum were purchased from Sigma. Ciprofloxacin hydrochloride (Cipro) was obtained from MP Biomedical Inc. PLGA (75:25) was purchased from Purac (Singapore). The B35 neuroblastoma cells line was gifted by Dr. Anita Quigley at St. Vincent's Hospital, Melbourne. Dulbecco's modified Eagle's medium (DMEM), fetal bovine serum (FBS), penicillin/streptomycin (Pen/Strep), Calcein AM, Alexa Fluor 546 anti-mouse secondary antibody, 4',6-diamidino-2-phenylindole (DAPI) and propidium iodide (PI) were purchased from Life Technologies (Melbourne, Australia). Anti-beta III tubulin primary antibody was obtained from Covance.

Preparation of PEDOT:PSS-CHI-PLGA fibers:

PEDOT:PSS pellets were dispersed in water at 25 mg/ml. Chitosan (CHI), as a biopolymer with amino groups that coagulates the PEDOT:PSS dispersion, was prepared at 1.0 wt.% in 2.0 wt.% acetic acid and used as the coagulation solution. A syringe pump (KDS-Scientific 100) was utilized to inject the PEDOT:PSS into CHI at a feed rate of 15 ml/h. 15 (wt/v)% of PLGA (75:25) was prepared in a 1:1 mixture of dichloromethane and dimethylformamide (DCM:DMF). The electrospinning of PLGA was performed with a feed rate of 1.0 ml/h, tip-to-collector distance of 30 cm and an applied potential of 15 kV. To produce PEDOT:PSS-CHI-PLGA films, similar concentrations of PEDOT:PSS and CHI solutions were cast on glass slides using spin coating, followed by electrospinning of the PLGA solution with the same spinning parameters as for fibers.

Fiber characterization methods:

The morphology of the fibers was characterized using a scanning electron microscope (JEOL JSM7500FA). The specimens for cross-sectional imaging were prepared by freezing the fibers in liquid nitrogen prior to fracture. The electrochemical properties of fibers was investigated via cyclic voltammetry (CV) in phosphate buffered saline (PBS, pH~7.4), in a three-electrode cell, using a platinum mesh counter electrode, an Ag/AgCl (3 M NaCl) reference electrode and both PEDOT:PSS-CHI and PEDOT:PSS-CHI-PLGA fibers as free-standing working electrodes. The electrochemical parameters were controlled using EChem software version 1.5 (EDAQ, Sydney). The mechanical properties of the fibers were evaluated using a Shimadzu tensile tester (EZ-S) at a strain rate of 0.5 %/min. The fibers were mounted on aperture cards (1.0 cm length window), fixed using commercial superglue and allowed to air dry.

Ciprofloxacin hydrochloride release measurement:

The release of Cipro was measured using UV-visible spectroscopy by determining the absorption of Cipro at its λ_{max} (270 nm) in PBS. The UV-visible spectra of Cipro in PBS solutions containing Cipro at varying concentrations were recorded between 200 nm and 300 nm using a Shimadzu UV

1601 spectrophotometer in order to construct a calibration curve at 270 nm for sample analysis.

Cell culture studies

The B35 neuroblastoma cell line was subcultured in DMEM supplemented with 10 (v/v) % FBS to passage 8-9. Subculturing was carried out at a split ratio of 1:5 at 70–80 % confluence. To seed cells onto fibers, cells were suspended at 15,000 cells/ml in DMEM supplemented with 10 % FBS and 1.0 % Pen/Strep. The fibers were placed onto glass slides in an aligned pattern and 4-well chambers were glued onto the glass slides using a cell-compatible silicon adhesive. The wells were sterilized by soaking in 70% (v/v) ethanol for 10 min. After complete drying of fibers in a sterile environment, cells were seeded and cultured at 37 °C in a humidified 5 % CO_2 environment for 24, 48 & 72 h prior to staining and imaging. In addition, cells were seeded at a density of 30,000 cells/ml on the fibers and differentiated by replacement of growth media with DMEM containing 1.0 % horse serum and 1.0 mM cAMP, the next day, then incubated for 24, 48 & 72 h with media replacement every 48 h.

Fluorescence staining and imaging of cells

Cells were incubated with 5.0 µM Calcein AM in growth media, for 15 min in the cell culture environment. Propidium iodide (PI) at 1 µg/ml was added during the 2 last min of staining. Culture media was replaced with PBS before images were captured using an AxioImager fluorescent microscope (Carl Zeiss) with AxioVision v. 4.8 software. Live and dead cells were stained bright fluorescent green and red respectively.

For immunofluorescence of differentiated cells, the cells were rinsed with with PBS. Cells were fixed using 3.7 % PFA for 10 min followed by rinsing with PBS. Cells were permeabilized with a 50:50 mixture of methanol:acetone on ice for 5 min followed by washing twice with PBS. Non-specific binding was blocked using 5% goat serum/PBS/0.1% Triton X-100) for 1 h at room temperature (RT). Cells were incubated with anti-βIII tubulin primary antibody diluted 1 in 1000 in blocking solution overnight at 4 °C followed, by washing with PBS twice. The secondary antibody (Alexa Fluor 546 anti-mouse) at 1 in 1000 in blocking solution was added and cells incubated at RT for 1 h followed by three PBS washes for 20 min each. Finally, cell nuclei were stained with DAPI (1 in 1000 in PBS) for 5 min at room temperature and the media was replaced with fresh PBS for imaging.

Cryo-SEM imaging of cells on the fibers

Cells were rinsed with PBS, then fixed using 3.7 % PFA for 10 min at RT, followed by washing and storage in PBS prior to imaging. Small 1x1 mm sections of the hydrated material were cut and drained of excess PBS and then placed onto a small (25 mm diam x 10 mm thick) brass block. This whole sample was then plunged into a liquid nitrogen bath for 45 to 50 secs, removed and transferred directly onto the stage of a JEOL 6490LV SEM. The samples were viewed at 10 mm working distance using BSE imaging mode at 15 kV operating voltage.

Cells viability assay

To study cell viability and proliferation on the fibers over time, cells were seeded onto fibers using the above protocol. Cells were incubated in growth media for 24, 48 & 72 h with media changes every 48 h. Cell Titer 96 AQ_{ueous} one solution cell proliferation kit from Promega (MTS assay) was used to estimate numbers of metabolically active cells. At each time point, 40 µl of the MTS reagent was added into each well and cells returned to the incubator for 3 h. Media was collected and the absorbance was compared to that of controls without cells at 490 nm using a Spectromax plate reader (Molecular Devices). A standard curve was prepared to ensure the linearity of the assay over the measured range of cell numbers.

Statistical test

Three independent experiments with triplicates for each sample were carried out. Statistical difference of the data was analyzed using one-way ANOVA with Tukey's post-hoc test at the 95 % significance level.

Results and discussion

Combined electrospinning and wet-spinning

The schematic presented in Figure 1 illustrates the combined electro- and wet-spinning method used to fabricate the multifunctional fibers with a core-sheath configuration and hierarchical structure to obtain fibers that can be combined into macroscopic structures. In this method, the conducting polymer PEDOT:PSS dispersion was injected into a coagulation bath containing chitosan to form the hybrid PEDOT:PSS-CHI fibers. The amino group in chitosan cross-links with the poly(styrenesulfonate) group in PSS to coagulate the fibers.[5] When the sulfonate groups in PSS cross-link with amino group in chitosan, they become insoluble in water. The fiber was then drawn through an ethanol wash bath at which point the PLGA nanofibers were simultaneously electrospun on top of the wash bath. As the PEDOT:PSS-CHI hybrid fiber was pulled from the ethanol bath, the electrospun PLGA nanofibers formed a unidirectional sheath coating onto it with a mean diameter of 1.64 ± 0.6 µm (Figure S1).

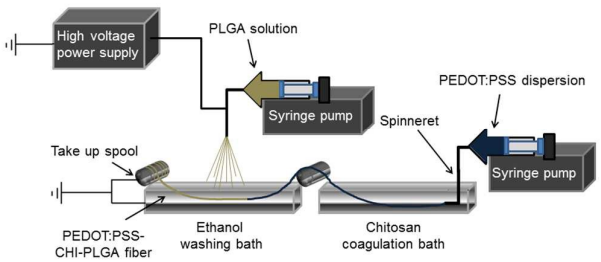

Figure 1. Schematic of combined wet and electrospinning method.

Conventional electrospun fibers show promise as artificial extracellular matrices in regenerative medicine however, they usually suffer from poor mechanical properties or difficulty in handling. The combined or hybrid PEDOT:PSS-CHI-PLGA electro-wet

spun fibers present a microscale solid wet-spun fiber contained within a layer of PLGA electrospun fibers with sub-micron features, that allow improved handling. This improved handling can facilitate the use of braiding and knitting processes for commercial production, while retaining their micron to sub-micron scale features for improved cell attachment.

Characterisation of PEDOT:PSS-CHI-PLGA fibers

Figure 2 shows SEM images of PEDOT:PSS-CHI-PLGA fibers demonstrating a coaxial configuration and hierarchical porosity with PLGA electrospun fibers surrounding the wet-spun PEDOT:PSS-CHI fiber. Cross-sectional SEM images of the composite fiber show micron and sub-micron electrospun

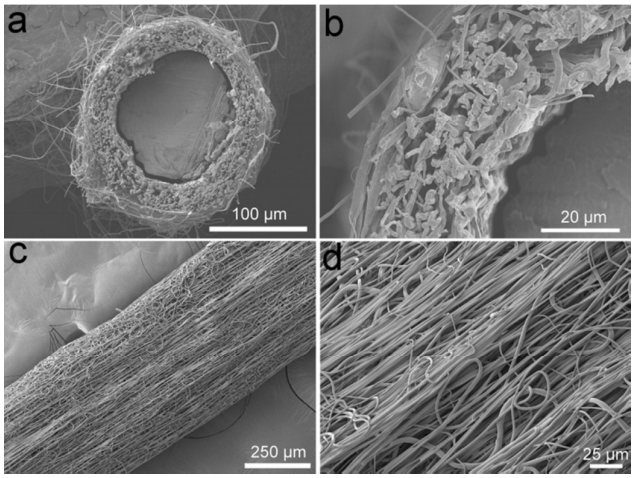

Figure 2. Scanning electron micrographs (SEM) of PEDOT:PSS-CHI-PLGA fiber. (a and b) SEM of the cross-section of the fiber. (C and d) SEM of the surface of the fiber.

fibers (Figures 2a and b) covering the micron size PEDOT:PSS-CHI fiber core. From Figures 2a and b, it appears that the electrospun fibers adhered well to the wet-spun fiber core with the slight separation observed due to sample preparation for SEM imaging. It was also observed that the electrospun fibers extended along the entire length of the wet-spun fibers (Figures 2c and d) and were mostly aligned with the direction of the wet-spun fiber. This alignment is due to mechanical forces applied to the electrospun nanofibers as the PEDOT:PSS-CHI fiber exits the wash bath, causing the electrospun PLGA fibers to be ordered in the direction of drawing (fiber axis). In order to quantitatively measure the alignment direction, Fast Fourier Transform (FFT) analysis of the SEM images was employed.[20] Directionality histograms (Figure S2) verify the alignment of PLGA electrospun fibers along the length of PEDOT:PSS-CHI core fiber.

The method outlined here can be used to spin unlimited lengths of aligned core-supported and oriented electrospun fibers. Moreover, the present method demonstrates that the porosity of the final structure was preserved (Figure 2d) given that ethanol is a volatile solvent, which allows the electrospun mat to solidify quickly and maintain its porosity.[38] At the same time, the core PEDOT:PSS-CHI wet-spun fibers provide mechanical strength to hold the structure together. When the ethanol evaporates and the fiber dries, the entanglement of the PLGA electrospun fibers prevents them from collapsing, resulting in a porous sheath. In contrast, PEDOT:PSS-CHI-PLGA 2D films had lower porosity and no alignment of fibers as a results of the preparation technique which causes the fibers to attached to one another as they are electrospun (data not shown).

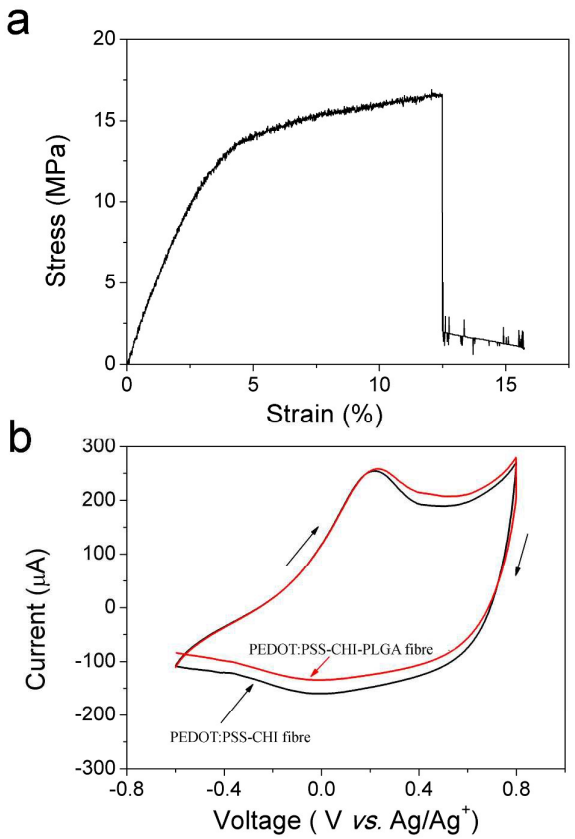

Figure 3. (a) Stress-strain curve of PEDOT:PSS-CHI-PLGA fiber, (b) cyclic voltammograms (CV) of electro and wet-spun PEDOT:PSS-CHI-PLGA and wet-spun PEDOT:PSS-CHI fiber in PBS (pH ~ 7.4) between – 0.6 and + 0.8 V at a scan rate of 25 mV/s. Arrows indicate the direction of the potential scan.

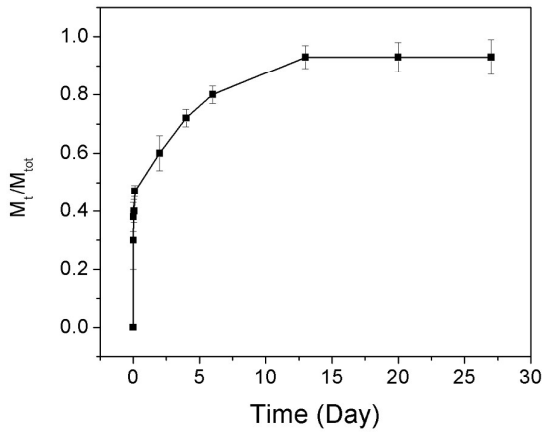

Figure 4. Cumulative release of Cipro from PEDOT:PSS-CHI-PLGA fiber into PBS at 37 °C. The M_t/M_{tot} represents the ratio of the released drug to the amount of loaded drug.

Mechanical and electrochemical properties

The micron-structured fibers were found to be mechanically robust (Figure 3a) giving a Young's modulus and ultimate stress of 420 MPa and 16.5 MPa, respectively, indicating that the fibers can be utilized as a self-supported electrode assembly.

Cyclic voltammetry (CV) of electro- and wet-spun PEDOT:PSS-CHI-PLGA fibers and PEDOT:PSS-CHI fibers (control) were performed in PBS (Figure 3b). Both scans show the oxidation and reduction peaks of PEDOT:PSS at +0.2 and -0.1 V, respectively, consistent with the redox behavior of PEDOT:PSS fibers previously reported,[5, 36, 37, 39, 40] which confirmed that the addition of the porous non-conducting PLGA layer had little impact on the electroactivity observed for the core fiber. The highly porous nature of the PLGA electrospun fiber architecture ensured that the conducting PEDOT:PSS-CHI fiber was accessible to the surrounding electrolyte. Conversely, when the PEDOT:PSS-CHI fiber was coated with a non-porous layer of PLGA (via dipping the PEDOT:PSS-CHI fiber into a solution of 15 wt/v% PLGA for a few seconds followed by drying), it was not possible to observe the electrochemical properties of the PEDOT:PSS-CHI fiber (data not shown) due to the PLGA layer being impermeable to the ions in the electrolyte, resulting in the composite fiber becoming completely insulating.

Ciprofloxacin release study

The multifunctional nature of the novel PEDOT:PSS-CHI-PLGA fiber was demonstrated by the incorporation of an antibacterial drug, ciprofloxacin hydrochloride (Cipro) into the electrospinning solution and subsequent release from the electrospun component. The presence of drug in the nanofibers was confirmed using Fourier Transform Infra-Red (FTIR) spectroscopy (Figure S5) and the release of the antibiotic from the fibers (PEDOT:PSS-CHI-PLGA-Cipro) was measured using UV-visible spectroscopy of the release media (see experimental section). Figure 4 shows the cumulative release profile of Cipro into PBS over 30 days. There was a burst release within the first hour followed by a sustained release over the next 14 days, by which time approximately 90 % of the incorporated drug had been released. Burst release is believed to result from the release of incorporated drug that is located close to the surface of the PLGA fibers whilst the release over longer times is from the diffusion of the drug that is incorporated deeper within the PLGA fibers.

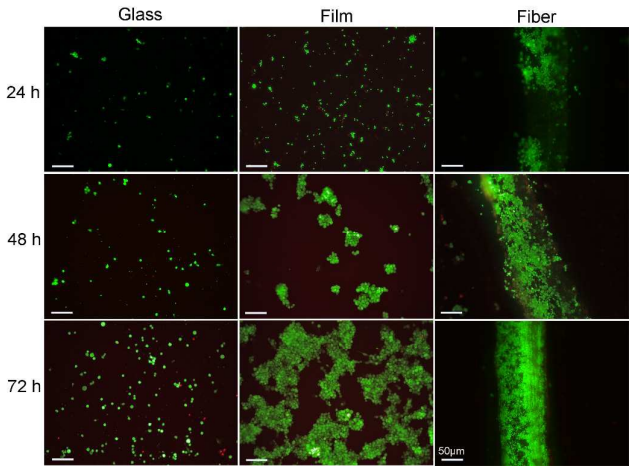

Figure 5. Representative images of B35 neuroblastoma cells on PEDOT:PSS-CHI-PLGA hybrid fibers, PEDOT:PSS-CHI-PLGA films and glass slides. Live and dead cells were visualised by fluorescence staining with calcein AM (green) and propidium iodide (PI) (red), respectively. Scale bars represent 50 µm for all images.

Cell studies

The introduction of sub-micron dimensional features to surfaces has been used previously to elicit different responses from the same cell phenotype.[40] Increasing the nanoscale roughness of the pores of scaffold walls has been found to increase cell attachment, proliferation and cellular expression of ECM components.[41] The electrospun PLGA fibers were therefore expected to improve cell attachment to the multifunctional structure.

Fluorescence staining of proliferating cells.

In order to evaluate the cell viability and attachment to the PEDOT:PSS-CHI-PLGA hybrid fibers, live/dead fluorescent staining of B35 neuroblastoma cells on the glass substrate, PEDOT:PSS-CHI-PLGA films and fibers was carried out. Figure 5 shows images of calcein/PI stained cells during three days of culture on all substrates. Proliferation rates were much higher on the hybrid films and fibers (see also Figure 6) compared to the glass substrate, which also had a low percentage of dead cells (red spots) by 72 h of culture. In the case of the hybrid fibers, almost all of the cells are oriented toward the fiber direction (see also Figure S4), while cells were randomly scattered on the glass surface and clustered on the films. Moreover, comparing 2D surfaces (glass and film) with the hybrid fibers (3D construct), the latter supported better cell attachment and migration along the hybrid fiber. This could be attributed to the presence of sub-micron features on the surface of the electrospun sheath.

In contrast to the hybrid fibers, when B35 cells were cultured for 72 h on the PEDOT:PSS-CHI fibers (without the PLGA electrospun layer), there was no observed cell adhesion onto the fibers and the cells were agglomerated on the underlying tissue culture substrate (see Figure S5). This highlights the effect of sub-micron structures and oriented PLGA fibers on the outside of the PEDOT:PSS-CHI conducting core to modify cell attachment to the fibers.

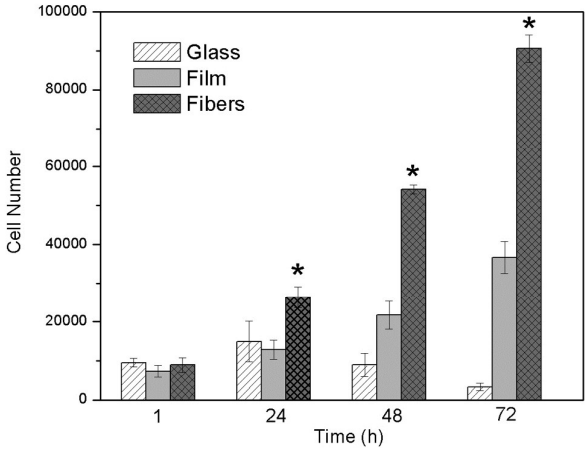

Figure 6. MTS assay indicating proliferation of seeded B35 neuroblastoma cells on PEDOT:PSS-CHI-PLGA hybrid fibers in comparison with PEDOT:PSS-CHI-PLGA films and glass slides over 72 h in culture. Error bars represent one standard error of the mean (n = 3), and the statistical significance was assessed by one-way ANOVA with Tukey's post-hoc test and reported with 95% (*) confidence.

Quantitation of cell proliferation.

Quantitative evaluation of the proliferation of B35 neuroblastoma cells on the hybrid fibers compared with that on flat surfaces (glass and film) was carried out using the MTS assay. Figure 6 demonstrates the trend of cell growth over three days. While, cell numbers progressively increased on PEDOT:PSS-CHI-PLGA fibers and films, cell viability started to decline after the first 24 h for cells in contact with the glass substrate (control). Although the seeded cell numbers were similar on all three substrates (1 h time point), population doubling times (PDT) on the PEDOT:PSS-CHI-PLGA fibers were shorter (21.2 h) over three days in culture, compared to the equivalent films (30.5 h). This may be due to the higher porosity and better cell attachment to the aligned PLGA electrospun fiber sheath around the PEDOT:PSS-CHI core, compared to the electrospun mat on the cast films. The results are in agreement with the fluorescence staining of B35 cells (Figure 5), showing higher cell densities when they are in contact with fibers rather than films. The results indicate the positive effect of the aligned micro-structured PLGA on both cell attachment and proliferation.

Fluorescence staining of differentiating B35 cells.

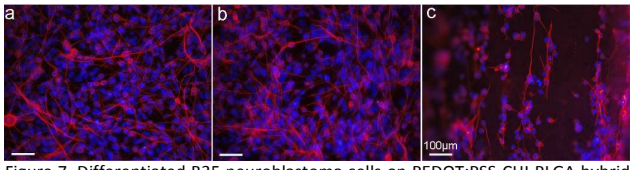

Figure 7. Differentiated B35 neuroblastoma cells on PEDOT:PSS-CHI-PLGA hybrid fibers in comparison with PEDOT:PSS-CHI-PLGA films and glass slides over 72 h in culture. a) glass, b) film, c) fibers. Cell nuclei were stained with DAPI (blue) and neurites immunostained for β-III tubulin (red). Scale bars represent 100 µm.

The differentiation of B35 cells on the PEDOT:PSS-CHI-PLGA fibers, films and the glass substrate were studied over a 72 h period (Figure 7). B35 cells possess long neurites in culture on all samples, however the percentage of cells extending neurites and expressing β-III tubulin was much higher on the fibers. In contrast to flat surfaces (glass and film), where there was no preferred direction of neurite elongation, on the hybrid fibers, cells extended their neurites along the fiber axis.

Quantitation of the length of the axons was not possible due to the cell migration into the interior of the electrospun shell. Figure 8 shows cryo-SEM images of differentiated B35 cells on the PEDOT:PSS-CHI-PLGA fibers. When the cells were differentiated on the hybrid fibers the extending neurites were observed to align with the nanofiber direction and the cells migrated into the electrospun shell (indicated by red arrows in Figure 8).

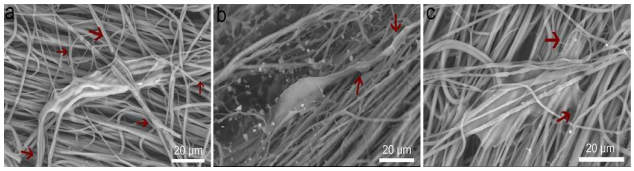

Figure 8. Cryo-SEM images of differentiated B35 cells on the PEDOT:PSS-CHI-PLGA fibers (the integration was so profound that the junction between cells and electrospun mat was indistinguishable at times (red arrows point to the axons on electrospun fibers. Scale bars represent 20 µm).

Since, alignment of neurites is fundamental to the structure of endogenous nerve, patterning of neuronal outgrowth *in vitro* is important for the development of models of neuronal behaviour as well as scaffolds for tissue engineering to aid in neuronal repair. These novel PEDOT:PSS-CHI-PLGA electro- and wet-spun fibers could potentially be used to control cell behavior using both their directionality and electroactive properties. The PLGA electrospun shell facilitated the attachment, proliferation, and aligned differentiation of B35 cells. Moreover, the porosity of the electrospun mat allowed cell migration into the structure and also facilitated ion exchange to the inner PEDOT:PSS-CHI conducting core.

Conclusions

The development of a facile method to continuously fabricate multifunctional fibers with controllable architecture and porosity is an essential step in the engineering of multifunctional AECM with suitable mechanical, electrochemical properties and also nerve cell compatibility. The present work demonstrates this versatility, which can be further developed to fabricate various biocompatible and conducting 3D constructs. The wet-spun PEDOT:PSS-CHI core fiber provides electrochemical activity and the PLGA electrospun fiber sheath facilitates cell attachment to the multifunctional structure by introduction of micron and sub-micron features onto the surface of the wet-spun fibers. The electroactivity, along with the cytocompatibility of the novel fibers show promise for fabricating electroactive AECM, which may be utilised to enhance the behaviour of electrically-responsive cells such as neural cells.

Acknowledgements

This work was supported by Australian Research Council (ARC) Centre of Excellence Scheme, Project Number CE 140100012 (RJ), ARC Queen Elizabeth II Fellowship (SEM), ARC Federation Fellowship (GGW), National Health and Medical Research

Council (NHMRC), Project No APP1065463 (DE), and was performed in part at the Materials Node of the Australian National Fabrication Facility (ANFF). The authors would like to thank the UOW Electron Microscopy Centre for providing the imaging facilities, Dr. Tony Romeo for cryo-SEM imaging, Dr. Patricia Hayes for FTIR assistance and Ms. Sue Ku for assistance in cell culture.

Notes and references

‡ Electronic Supplementary Information (ESI) available: [Supporting figures S1 to S8]. See DOI: 10.1039/c000000x/

1. P. Bajaj, R. M. Schweller, A. Khademhosseini, J. L. West and R. Bashir, *Annu. Rev. Biomed. Eng.*, 2014, **16**, 247-276.
2. A. Khademhosseini, J. P. Vacanti and R. Langer, *Scientific American*, 2009, **300**, 64 - 71
3. D. Grafahrend, K.-H. Heffels, M. V. Beer, P. Gasteier, M. Möller, G. Boehm, P. D. Dalton and J. Groll, *Nat Mater*, 2011, **10**, 67-73.
4. W.-G. Bae, J. Kim, Y.-H. Choung, Y. Chung, K. Y. Suh, C. Pang, J. H. Chung and H. E. Jeong, *Biomaterials*, 2015, **69**, 158-164.
5. D. Esrafilzadeh, J. M. Razal, S. E. Moulton, E. M. Stewart and G. G. Wallace, *J Control Release*, 2013, **169**, 313-320.
6. M. Zhu, Z. Wang, J. Zhang, L. Wang, X. Yang, J. Chen, G. Fan, S. Ji, C. Xing, K. Wang, Q. Zhao, Y. Zhu, D. Kong and L. Wang, *Biomaterials*, 2015, **61**, 85-94.
7. Z. Wang, Y. Cui, J. Wang, X. Yang, Y. Wu, K. Wang, X. Gao, D. Li, Y. Li, X.-L. Zheng, Y. Zhu, D. Kong and Q. Zhao, *Biomaterials*, 2014, **35**, 5700-5710.
8. H. J. Diao, W. C. Low, Q. R. Lu and S. Y. Chew, *Biomaterials*, 2015, **70**, 105-114.
9. C. J. Luo, S. D. Stoyanov, E. Stride, E. Pelan and M. Edirisinghe, *Chem. Soc. Rev.*, 2012, **41**, 4708-4735.
10. M. Kobayashi, N. Y. Lei, Q. Wang, B. M. Wu and J. C. Y. Dunn, *Biomaterials*, 2015, **61**, 75-84.
11. C. P. Grey, S. T. Newton, G. L. Bowlin, T. W. Haas and D. G. Simpson, *Biomaterials*, 2013, **34**, 4993-5006.
12. L. Natarajan, J. New, A. Dasari, S. Yu and M. A. Manan, *RSC Advances*, 2014, **4**, 44082-44088.
13. W. Liu, S. Thomopoulos and Y. Xia, *Adv. Health. Mater.*, 2012, **1**, 10-25.
14. C. Zhang, H. Yuan, H. Liu, X. Chen, P. Lu, T. Zhu, L. Yang, Z. Yin, B. C. Heng, Y. Zhang and H. Ouyang, *Biomaterials*, 2015, **53**, 716-730.
15. T. Dvir, B. P. Timko, D. S. Kohane and R. Langer, *Nat. Nanotechnol.*, 2011, **6**, 13-22.
16. P. Ke, X.-N. Jiao, X.-H. Ge, W.-M. Xiao and B. Yu, *RSC Advances*, 2014, **4**, 39704-39724.
17. J. A. Matthews, G. E. Wnek, D. G. Simpson and G. L. Bowlin, *Biomacromolecules*, 2002, **3**, 232-238.
18. A. Moradzadegan, S.-O. Ranaei-Siadat, A. Ebrahim-Habibi, M. Barshan-Tashnizi, R. Jalili, S.-F. Torabi and K. Khajeh, *Eng. Life Sci.*, 2010, **10**, 57-64.
19. D. Esrafilzadeh, M. Morshed and H. Tavanai, *Synthetic Metals*, 2009, **159**, 267-272.
20. R. Jalili, M. Morshed and S. A. H. Ravandi, *J. Appl. Polym. Sci.*, 2006, **101**, 4350-4357.
21. D. Esrafilzadeh, R. Jalili and M. Morshed, *J. Appl. Polym. Sci.*, 2008, **110**, 3014-3022.
22. F. Yang, R. Murugan, S. Wang and S. Ramakrishna, *Biomaterials*, 2005, **26**, 2603-2610.
23. Z. Yin, X. Chen, J. L. Chen, W. L. Shen, T. M. Hieu Nguyen, L. Gao and H. W. Ouyang, *Biomaterials*, 2010, **31**, 2163-2175.
24. X. Zong, H. Bien, C.-Y. Chung, L. Yin, D. Fang, B. S. Hsiao, B. Chu and E. Entcheva, *Biomaterials*, 2005, **26**, 5330-5338.
25. R. D. Breukers, K. J. Gilmore, M. Kita, K. K. Wagner, M. J. Higgins, S. E. Moulton, G. M. Clark, D. L. Officer, R. M. I. Kapsa and G. G. Wallace, *J. Biomed. Mater. Res. A*, 2010, **95A**, 256-268.
26. I. Tonazzini, E. Jacchetti, S. Meucci, F. Beltram and M. Cecchini, *Advanced Healthcare Materials*, 2015, **4**, 1849-1860.
27. X. Li, H. Liang, J. Sun, Y. Zhuang, B. Xu and J. Dai, *Advanced Healthcare Materials*, 2015, **4**, 1869-1876.
28. C. P. Barnes, S. A. Sell, E. D. Boland, D. G. Simpson and G. L. Bowlin, *Adv. Drug Deliv. Rev.*, 2007, **59**, 1413-1433.
29. D. R. Nisbet, J. S. Forsythe, W. Shen, D. I. Finkelstein and M. K. Horne, *J. Biomater. Appl.*, 2009, **24**, 7-29.
30. X. Yang, J. D. Shah and H. Wang, *Tissue Eng. A.*, 2009, **15**, 945-956.
31. A. F. Quigley, J. M. Razal, M. Kita, R. Jalili, A. Gelmi, A. Penington, R. Ovalle-Robles, R. H. Baughman, G. M. Clark, G. G. Wallace and R. M. I. Kapsa, *Adv. Health. Mater.*, 2012, **1**, 801-808.
32. J. Thunberg, T. Kalogeropoulos, V. Kuzmenko, D. Hägg, S. Johannesson, G. Westman and P. Gatenholm, *Cellulose*, 2015, **22**, 1459-1467.
33. K. Krukiewicz, A. Stokfisz and J. K. Zak, *Mater. Sci. Eng. C.*, 2015, **54**, 176-181.
34. R. T. Richardson, A. K. Wise, B. C. Thompson, B. O. Flynn, P. J. Atkinson, N. J. Fretwell, J. B. Fallon, G. G. Wallace, R. K. Shepherd, G. M. Clark and S. J. O'Leary, *Biomaterials*, 2009, **30**, 2614-2624.
35. R. Jalili, J. M. Razal and G. G. Wallace, *Sci. Rep.*, 2013, **3**.
36. R. Jalili, J. M. Razal and G. G. Wallace, *J. Mater. Chem.*, 2012, **22**, 25174-25182.
37. R. Jalili, J. M. Razal, P. C. Innis and G. G. Wallace, *Adv. Funct. Mater.*, 2011, **21**, 3363-3370.
38. P. Innocenzi, L. Malfatti, S. Costacurta, T. Kidchob, M. Piccinini and A. Marcelli, *J. Phys. Chem. A*, 2008, **112**, 6512-6516.
39. M. R. Abidian and D. C. Martin, *Adv. Funct. Mater.*, 2009, **19**, 573-585.
40. M. M. Stevens and J. H. George, *Science*, 2005, **310**, 1135-1138.
41. M. A. Pattison, S. Wurster, T. J. Webster and K. M. Haberstroh, *Biomaterials*, 2005, **26**, 2491-2500.